

Red Mud Minimisation and Management for the Alumina Industry by the Carbonation Method

A thesis submitted in fulfilment of
the requirement for the degree of

Doctor of Philosophy
Environmental Engineering

By **CUONG PHUOC TRAN**

February 2016



THE UNIVERSITY
of ADELAIDE

School of Chemical Engineering
Faculty of Engineering, Computer and Mathematical Sciences
The University of Adelaide

DECLARATION

I certify that this work contains no material which has been accepted for the award of any other degree or diploma in my name, in any university or other tertiary institution and, to the best of my knowledge and belief, contains no material previously published or written by another person, except where due reference has been made in the text. In addition, I certify that no part of this work will, in the future, be used in a submission in my name, for any other degree or diploma in any university or other tertiary institution without the prior approval of the University of Adelaide and where applicable, any partner institution responsible for the joint-award of this degree.

I give consent to this copy of my thesis, when deposited in the University Library, being made available for loan and photocopying, subject to the provisions of the Copyright Act 1968.

I also give permission for the digital version of my thesis to be made available on the web, via the University's digital research repository, the Library Search and also through web search engines, unless permission has been granted by the University to restrict access for a period of time.

CUONG PHUOC TRAN

Adelaide, 2016

ACKNOWLEDGEMENTS

This thesis has been a truly exciting and extremely enriching experience for me, both academically and personally. The outcomes of the research had the assistance and cooperation of many individuals and organisations. I would like to offer my grateful thanks to all of them. Particularly, I am thankful to the University of Adelaide and the Vietnamese Government for offering me a prestigious scholarship with which to conduct this study.

My special thanks must first go to my supervisor Associate Professor Dzuy Nguyen, for his continuous assistance, guidance, active supervision, and kindness to support me during my research candidature. He guided me initially on comprehensive research of materials and encouraged me since the early stages of research. I am greatly indebted to Associate Professor Dzuy Nguyen.

I would also like to express my appreciation to Associate Professor Brian O'Neill, who was my previous co-supervisor and initially helped me in critical thinking, supported and corrected my English at the beginning of this project. I am also thankful to Associate Professor Yung Ngothai, who replaced my previous co-supervisor in 2014. She always encouraged and shared with me difficulties occurring during the research. She provided me with the best facilities from her lab for my experiments.

My sincere thanks also go to Professor Allan Pring from Museum of South Australia, who provided me with permission to use facilities in SA Museum. My heartfelt thanks go to all academic members, office staff and other PhD students in the School of Chemical Engineering, School of Physical Sciences, and Adelaide Microscopy for their helps, friendship, encouragement, and understandings on many occasions. My grateful thanks go to my colleagues, who shared with me their research experience and made me feel confident through their talks and

companionship. It has been a memorable time of my life and one that I will never forget. I also thank Rio Tinto Alcan for kindly donating the red mud sample used in this study.

To my family members, who gave support from the beginning, I have greatly appreciated it and will try to do all those things that I promised. I would like to thank my lovely wife, Loan Thi Thuy Nguyen, for her love, inspiration, and endless encouragement. She has gracious and much patience in looking after our two lovely and gentle children, Vy Thuy Tran and Trong Phuoc Tran (Ken Tran). Their love and affection kept me sane during my research in Adelaide. Finally, I am thankful to my parents and my siblings for their unconditional love and constant prayers, as well as my parents-in-law, for their great understanding and support.

Adelaide, 2016

ABSTRACT

Bauxite residue (red mud), a waste from the Bayer process for refining bauxite to alumina, is highly alkaline (pH~13) and its treatment and management have posed environmental challenges to the alumina industry. Carbonation of red mud using carbon dioxide (CO₂) has previously been demonstrated to be feasible in both permanently capturing the CO₂ and neutralising this solid waste. A systematic study of the neutralisation of red mud by CO₂ over a range of different operating conditions is essential in order to optimise the carbonation process and maximise the volume of CO₂ captured by red mud.

The objectives of this study were to determine the acid neutralisation capacity of red mud and its solid and aqueous phase contribution to the acid neutralisation capacity via the analyses of red mud compositions. A red mud sample, provided by Rio Tinto Alcan, was carbonated in a range of different operating conditions with the intent of establishing the optimal condition for the carbonation process. The carbonation was carried out at room temperature and atmospheric pressure using a stirred tank reactor operating at different conditions such as total gas flow rate, CO₂ concentrations, stirring speeds, and solids concentrations in red mud. A range of analytical techniques such as X-ray diffraction (XRD), scanning electron microscopy (SEM) coupled with Energy Dispersive X-ray (EDX), Inductively Coupled Plasma Mass Spectrometry (ICP-MS) and Carbon-Hydrogen-Nitrogen Elemental Analyser (CHN) were used to ascertain the different mineral phases, change of chemical composition before and after carbonation, and carbonation capacity of the mud. Finally, based on the information of red mud composition, an equilibrium chemical model using MINEQL+ version 5.0 was developed for the carbonation process.

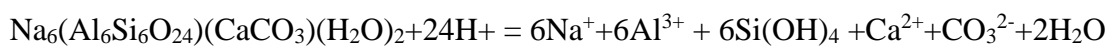
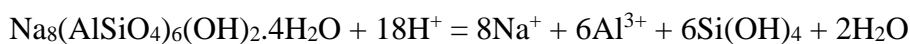
The acid neutralisation capacity of red mud was measured by both rapid and long-term titration of red mud slurries to pH endpoint of 4.5, 6, 8, and 10. At the endpoint of pH 4.5 corresponding to the bicarbonate endpoint, the acid neutralisation capacity of the red mud was found to be 0.79 and 1.91 meq/g red mud for rapid and long-term titration, respectively. Furthermore, it is estimated that the solid phase contributed approximately 81% to the acid neutralisation capacity, while contribution from the liquid phase was only 19% in the final long-term acid neutralisation capacity determination.

The carbonation process was observed to be significantly dependent on concentration of CO₂, total gas flow rate and stirring speeds, whereas the concentration of solids in red mud seemed to have a little effect based on only three concentrations studied. For the carbonation of red mud slurry, it took from 30-75 minutes to establish the equilibrium pH of 7.5-6.6 in the range of CO₂ concentrations of 10%-100%. In contrast, when the carbonation of red mud liquor only was performed at the same range of CO₂ values, the stable pH of 7.0-6.3 (0.3-0.5 pH unit lower) was reached within 15-30 minutes. After carbonation, the pH from carbonated red mud slurries, exposed to atmosphere CO₂, rebound quickly and took about 20-25 days to reach pH of 9.7. The carbonated liquor, however, showed a lower rate of pH recovery, and took a month to equilibrate to pH of 9.7.

The XRD patterns of carbonated red mud revealed the appearance of calcite and the increase of gibbsite due to the dissolution of sodalite and the breakdown of cancrinite minerals in the carbonation of red mud. The quantifications confirmed the precipitation of calcite from 0% to 1.51%, and the increase of gibbsite from 1.04% to 5.15% in raw red mud and carbonated red mud, respectively. XRD patterns and the quantifications associated with other results such as EDX and CHN analyses

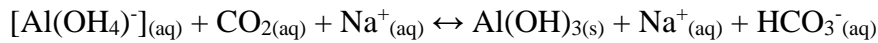
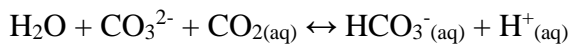
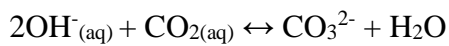
indicated that the most optimal conditions for carbonation process were 30% CO₂ concentration and total gas flow rate of 200mL/min. At this condition, the amount of CO₂ captured for the whole red mud (both solid and liquid phases) was highest at 65g CO₂/kg of red mud, and the alkalinity decreased from 11,610mg/L to 2,104mg/L as CaCO₃. Stirring speeds were found to be effective in boosting the extent of red mud carbonation and the amount of CO₂ sequestration. The results showed that when stirring speeds rose from 250rpm to 700rpm, the amount of CO₂ sequestration increased by 3.4g/kg of red mud, from 65 to 68.4g CO₂/kg of red mud.

The simulation for heavy metals dissolved in long-term titration of red mud at different pH levels of 4.5, 6, 8, 10, and 12.5 was performed using chemical equilibrium modelling system MINEQL+ 5.0. The modelling suggested that four key dominant metals Al, Na, Ca, and Fe were found to govern the aqueous chemistry of the red mud carbonation process due to their presence in both soluble and solid forms in red mud. Measured metal concentrations from long-term titration at various pH values indicated that boehmite (AlO(OH)) and hematite (Fe₂O₃) did not dissolve in the system, therefore, both Al and Fe were not responsible for the control of carbonation process as their concentrations remained unchanged. However, Na and Ca were considered the major solids controlling the process. The dissolution of sodalite (Na₈(AlSiO₄)₆(OH)₂·4H₂O) and cancrinite (Na₆(AlSiO₄)₆(CaCO₃)(H₂O)₂) were attributable to Na and Ca concentrations in the system. The key reactions are as below:



For carbonation process, a chemical model was formulated in MINEQL+ 5.0 to calculate the final equilibrium pH values for both carbonation of RM slurry and RM liquor at different concentration of CO₂. The results revealed that the simulated pH values for the carbonation process at different P_{CO₂} were 0.3-0.45 pH units higher than the experimental pH values. In other words, the difference in final pH equilibrium values between experimental and simulated carbonation of red mud varies from 4.0-6.0%. This difference is about 2 times lower than that of previous work done by Khaitan (2009b). The key reactions of carbonation of red mud are as follows:

Liquid phase reactions:



Solid phase reactions:

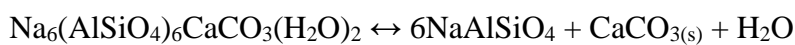
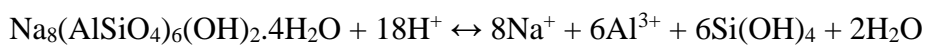


TABLE OF CONTENTS

DECLARATION	i
ACKNOWLEDGEMENTS	ii
ABSTRACT.....	iv
TABLE OF CONTENTS	viii
LIST OF FIGURES	xi
LIST OF TABLES	xvii
CHAPTER 1 INTRODUCTION.....	1
1.1. Background	1
1.2. Objectives	6
1.3. Organisation of Thesis.....	7
CHAPTER 2 LITERATURE REVIEW.....	8
2.1. Overview of Bauxite Residue Management.....	8
2.1.1. Bauxite Residue Generation Process	8
2.1.2. Physicochemical and Mineralogical Properties of Red Mud.....	11
2.1.3. Methods Utilised for Disposal of Red Mud.....	14
2.2. The Red Mud Utilisation Options	20
2.2.1. The Utilisations of Red Mud in Construction.....	21
2.2.2. The Utilisations of Red Mud in Chemical Applications.....	22
2.2.3. The Utilisations of Red Mud in Metallurgy.....	23
2.2.4. The Utilisations of Red Mud in Agriculture	24
2.2.5. The Utilisations of Red Mud in Environmental Treatment	26
2.3. Red Mud Neutralisation Methods	28
2.3.1. Neutralisation of Red Mud with Seawater.....	29
2.3.2. Neutralisation with Gypsum ($\text{CaSO}_4 \cdot 2\text{H}_2\text{O}$)	30
2.3.3. Neutralisation of Red Mud by Acid Mine Wastes.....	31
2.3.4. Neutralisation of Red Mud Using Mineral Acid	32
2.3.5. Neutralisation of Red Mud by Fly Ash.....	33
2.3.6. Neutralisation of Red Mud by Carbon Dioxide (CO_2) Gas	33
2.3.7. Perspectives of Red Mud Carbonation	35
2.3.8. Mechanism of the Carbonation of Red Mud	42
2.4. Summary	45

CHAPTER 3	MATERIALS AND METHODS	49
3.1.	Materials	49
3.2.	Materials Preparation	50
3.3.	Methods	50
3.3.1.	Acid Titration Procedures	50
3.3.2.	Determination of Total Alkalinity of Raw RM and Carbonated RM.....	52
3.3.3.	X-ray Diffraction (XRD)	53
3.3.4.	Scanning Electronic Microscopy and Energy Dispersive X-ray (SEM-EDX).....	53
3.3.5.	Carbon-Hydrogen-Nitrogen Elemental Analyser	54
3.3.6.	Thermal Analysis (TGA-DSC).....	55
3.3.7.	Fourier Transform Infrared Spectroscopy (FT-IR).....	55
3.4.	Carbonation Experiments	56
3.4.1.	Construction of Reaction Chamber.....	56
3.4.2.	Carbonation of RM	58
3.4.3.	pH Rebound of the Carbonated Red Mud	59
3.5.	Chemical Equilibrium Modelling.....	59
CHAPTER 4	RESULTS AND DISCUSSIONS	62
4.1.	Acid Neutralising Capacity (ANC) of the raw RM.....	62
4.1.1.	Rapid Titration of RM slurry and RM liquor	62
4.1.2.	Long Term Titration of Red Mud	64
4.2.	Carbonation of Red Mud	68
4.2.1.	Effect of CO ₂ Concentration on Carbonation of RM	68
4.2.2.	Effect of Total Gas Flow Rate on Carbonation of RM.....	72
4.2.3.	Effect of Stirring Speed on Carbonation of RM.....	74
4.2.4.	Effect of Solids Concentrations in RM on Carbonation of RM	76
4.2.5.	pH Rebound in Carbonated RM	78
4.2.6.	Longer Carbonation of RM.....	80
4.3.	Mineralogical Characterisation of Red Mud and Carbonated Red Mud.....	84
4.3.1.	X-ray Diffraction Analysis	84
4.3.2.	Micro-morphological Characterisation of raw RM and Carbonated RM by SEM	96
4.3.3.	Chemical Composition Changes by EDX	99
4.3.4.	Determination of Alkalinity of RM and Carbonated RM.....	111

4.3.5. Thermal Analysis using TGA-DSC.....	113
4.3.6. FT-IR Spectroscopy.....	115
4.4. Determination of CO ₂ Sequestration.....	116
4.4.1. Determination of CO ₂ sequestered in 2-hour carbonation of RM.....	116
4.4.2. Determination of CO ₂ sequestered in 5-day carbonation of RM.....	118
4.5. Modelling of Carbonation Process.....	122
4.5.1. Modelling of potentially dissolved metals.....	123
4.5.2. Modelling of RM carbonation.....	130
4.6. Summary.....	136
CHAPTER 5 FINDING OUTCOMES AND CONCLUSIONS.....	138
5.1. Major Findings of This Research.....	138
5.1.1. Acid Neutralisation Capacity (ANC) of Red Mud.....	138
5.1.2. Carbonation of Bauxite Residue.....	139
5.1.3. Modelling of the Carbonation Process.....	142
5.2. Conclusions.....	144
CHAPTER 6 RECOMMENDATIONS FOR THE FUTURE WORK.....	146
REFERENCES.....	147
APPENDIX.....	165

LIST OF FIGURES

Figure 1.1. Global production rate and cumulative inventory	2
Figure 2.1. Schematic of a general Bayer process	9
Figure 2.2. Lagooning red mud disposal.....	16
Figure 2.3. Schematic of dry stacking system.....	19
Figure 2.4. A possible flowsheet for recovery of Fe, Al, and Ti from bauxite residue	24
Figure 3.1. Carbonation reaction chamber	57
Figure 3.2. The experimental apparatus system for carbonation of RM.....	58
Figure 4.1. Rapid RM liquor titration compared with that of RM slurry (44% wt)....	63
Figure 4.2. Long-term titration of RM	64
Figure 4.3. XRD pattern of raw RM overlapped with titrated RM at pH 6	67
Figure 4.4. XRD pattern of raw RM overlapped with titrated RM at pH 4.5	67
Figure 4.5. Carbonation of RM slurry at different CO ₂ concentrations, fixed TF of 200mL/min and stirring speed of 250rpm.....	69
Figure 4.6. Carbonation of RM liquor at different CO ₂ concentrations, fixed TF of 200mL/min and stirring speed of 250rpm.....	69
Figure 4.7. Comparison of carbonation between RM slurry and RM liquor at some different CO ₂ concentrations, fixed TF of 200mL/min and stirring speed of 250rpm	70
Figure 4.8. Carbonation rate constant (k) for both RM slurry and RM liquor at different CO ₂ concentration, total gas flow rate 200mL/min and speed 250rpm	72
Figure 4.9. Carbonation of red mud by 30% of CO ₂ , 250rpm and different TF of gas	73
Figure 4.10. Carbonation rate constant (k) for RM slurry at 30% CO ₂ concentration, stirring speed 250rpm, and different total gas flow rate	74

Figure 4.11. Carbonation of red mud by 30% of CO ₂ , TF of 200mL/min and different stirring speeds	75
Figure 4.12. Rate constant (k) for carbonation of RM slurry by 30% CO ₂ concentration, TF of 200mL/min and different stirring speeds	76
Figure 4.13. Carbonation of red mud by 30% of CO ₂ , TF of 200mL/min and stirring speed of 250rpm, and different solids concentrations in RM	77
Figure 4.14. Rate constant (k) for carbonation of RM slurry by 30% CO ₂ concentration, TF of 200mL/min, and different solids concentrations in RM.....	78
Figure 4.15. pH rebound for both RM slurry and liquor at three CO ₂ concentrations, TF of 200mL/min, stirring speed of 250rpm	79
Figure 4.16. pH rebound of carbonated RM slurries at different solids concentrations	80
Figure 4.17. Longer carbonation of RM slurry at different CO ₂ concentrations	81
Figure 4.18. Longer carbonation of RM slurry at fixed 30% CO ₂ , stirring speed of 250rpm and at different total gas flow rate	82
Figure 4.19. Longer carbonation of RM slurry at fixed 30% CO ₂ , total gas flow rate of 200mL/min and different stirring speeds.....	83
Figure 4.20. Longer carbonation of RM slurry at fixed 30% CO ₂ , total gas flow rate of 200mL/min, stirring speeds of 250rpm and different solids concentrations of RM	83
Figure 4.21. Variation of powder XRD pattern of raw RM.....	84
Figure 4.22. Phase composition quantification of raw RM	85
Figure 4.23. XRD pattern of carbonated RM compared with raw RM.....	86
Figure 4.24. Phase composition quantification of carbonated RM at 15% CO ₂ concentration and total gas flow rate of 200mL/min	88
Figure 4.25. Phase composition quantification of carbonated RM at 30% CO ₂ concentration and total gas flow rate of 200mL/min	89
Figure 4.26. Phase composition quantification of carbonated RM at 40% CO ₂ concentration and total gas flow rate of 200mL/min	90

Figure 4.27. Phase composition quantification of carbonated RM at 60% CO ₂ concentration and total gas flow rate of 200mL/min	90
Figure 4.28. Phase composition quantification of carbonated RM at fixed 30% CO ₂ concentration and total gas flow rate of 100mL/min	91
Figure 4.29. Phase composition quantification of carbonated RM at fixed 30% CO ₂ concentration and total gas flow rate of 300mL/min	92
Figure 4.30. Phase composition quantification of carbonated RM at fixed 30% CO ₂ concentration and total gas flow rate of 400mL/min	93
Figure 4.31. Phase composition quantification of carbonated RM at fixed 30% CO ₂ concentration and stirring speed of 350rpm.....	94
Figure 4.32. Phase composition quantification of carbonated RM at fixed 30% CO ₂ concentration and stirring speed of 500rpm.....	95
Figure 4.33. Phase composition quantification of carbonated RM at fixed 30% CO ₂ concentration and stirring speed of 700rpm.....	95
Figure 4.34. SEM imaging of raw RM: (a) Sodalite in “cotton ball” form, and (b) Structure of crystalline sodalite.....	96
Figure 4.35. SEM imaging of carbonated RM at different CO ₂ concentration, TF of 200mL/min and stirring speed of 250rpm.....	98
Figure 4.36. The amounts of C and CO ₂ absorbed by RM after 2-hour carbonation at different CO ₂ concentration, TF of 200mL/min and stirring speed of 250rpm	101
Figure 4.37. Amounts of C and CO ₂ absorbed by RM after 5-day carbonation	103
Figure 4.38. Amounts of C and CO ₂ absorbed by RM at a given 30% CO ₂ concentration, 250rpm and different TF of gas.....	105
Figure 4.39. Amounts of C and CO ₂ absorbed by RM at given 30% CO ₂ , TF of 200mL/min and different stirring speeds	106
Figure 4.40. Amounts of C and CO ₂ captured by RM in different solids concentrations	109

Figure 4.41. Comparison of amounts of C and CO ₂ captured between 2-hour and 5-day carbonation at fixed TF of 200mL/min, 250rpm and different CO ₂ concentrations	111
Figure 4.42. Changes in HCO ₃ ⁻ , CO ₃ ²⁻ , and OH ⁻ alkalinity in raw RM and carbonated RM at different concentrations of CO ₂ , TF of 200mL/min, 250rpm	112
Figure 4.43. Acid titration curves for a) Raw RM and b) Carbonated RM at 30% CO ₂ , TF of 200mL/min and stirring speed of 250rpm.....	113
Figure 4.44. TGA-DSC plots indicating weight loss of RM	114
Figure 4.45. TGA-DSC plots indicating weight loss of carbonated RM.....	115
Figure 4.46. Fourier Transform Infrared (FT-IR) spectra of RM and carbonated RM	116
Figure 4.47. Amounts of CO ₂ sequestered by RM after 2-hour carbonation at different CO ₂ concentrations, stirring speed of 250rpm	117
Figure 4.48. Amounts of CO ₂ captured by RM (A): solid, (B): liquor, after 5-day carbonation at different CO ₂ concentrations, TF of 200mL/min and speed of 250rpm	119
Figure 4.49. Comparison of CO ₂ amounts captured between 2-hour and 5-day carbonations	120
Figure 4.50. Amounts of CO ₂ captured by RM carbonated 30% CO ₂ concentration, TF of 200mL/min and at different stirring speeds	120
Figure 4.51. Amounts of CO ₂ captured by RM with different solids concentrations carbonated at 30% CO ₂ concentration, TF of 250mL/min and 250rpm	121
Figure 4.52. Metal concentrations in RM liquor as a function of pH	124
Figure 4.53. Comparison of simulated and experimental carbonation of RM liquor at different CO ₂ concentration and TF of (A): 100mL/min, (B): 200mL/min.....	133
Figure 4.54. Comparison of simulated and experimental carbonation of RM liquor at different CO ₂ concentration and TF of (C): 300mL/min, (D): 400mL/min.....	133
Figure 4.55. Comparison of simulated and experimental carbonation of RM slurry at different CO ₂ concentration and TF of (A): 100mL/min, (B): 200mL/min.....	134

Figure 4.56. Comparison of simulated and experimental carbonation of RM slurry at different CO ₂ concentration and TF of (C): 300mL/min, (D): 400mL/min.....	134
Figure B-1. Carbonation of RM slurry at different CO ₂ concentrations, fixed TF of 100mL/min and stirring speed of 250rpm.....	172
Figure B-2. Carbonation of RM slurry at different CO ₂ concentrations, fixed TF of 300mL/min and stirring speed of 250rpm.....	172
Figure B-3. Carbonation of RM slurry at different CO ₂ concentrations, fixed TF of 400mL/min and stirring speed of 250rpm.....	172
Figure B-4. Carbonation of RM liquor at different CO ₂ concentrations, fixed TF of 100mL/min and stirring speed of 250rpm.....	173
Figure B-5. Carbonation of RM liquor at different CO ₂ concentrations, fixed TF of 300mL/min and stirring speed of 250rpm.....	173
Figure B-6. Carbonation of RM liquor at different CO ₂ concentrations, fixed TF of 400mL/min and stirring speed of 250rpm.....	173
Figure B-7. Carbonation of RM by 25% CO ₂ at different TF of gas.....	174
Figure B-8. Carbonation of RM by 40% CO ₂ at different TF of gas.....	174
Figure B-9. Carbonation of RM by 50% CO ₂ at different TF of gas.....	174
Figure B-10. Carbonation of red mud by 30% of CO ₂ , TF of 100mL/min at different stirring speeds	175
Figure B-11. Carbonation of red mud by 30% of CO ₂ , TF of 300mL/min at different stirring speeds	175
Figure B-12. Carbonation of red mud by 30% of CO ₂ , TF of 400mL/min at different stirring speeds	175
Figure B-13. Carbonation of red mud by 30% of CO ₂ , TF of 100mL/min, stirring speed 250rpm at different solid concentrations of RM.....	176
Figure B-14. Carbonation of red mud by 30% of CO ₂ , TF of 300mL/min, stirring speed 250rpm at different solid concentrations of RM.....	176
Figure B-15. Carbonation of red mud by 30% of CO ₂ , TF of 400mL/min, stirring speed 250rpm at different solid concentrations of RM.....	176

Figure B-16. Carbonation of red mud by 40% of CO ₂ , TF of 200mL/min, stirring speed 250rpm at different solid concentrations of RM.....	177
Figure B-17. Carbonation of red mud by 30% of CO ₂ , TF of 200mL/min, stirring speed 350rpm at different solid concentrations of RM.....	177
Figure B-18. Carbonation of red mud by 30% of CO ₂ , TF of 200mL/min, stirring speed 500rpm at different solid concentrations of RM.....	177
Figure B-19. Carbonation of red mud by 30% of CO ₂ , TF of 200mL/min, stirring speed 700rpm at different solid concentrations of RM.....	178
Figure B-20. pH rebound for both RM slurry and liquor at some CO ₂ concentrations, TF of 200mL/min, stirring speed of 250rpm	178
Figure C-1. Phase composition quantification of carbonated RM at 20% CO ₂ concentration, total gas flow rate 200mL/min	200
Figure C-2. Phase composition quantification of carbonated RM at 50% CO ₂ concentration, total gas flow rate 200mL/min	201

LIST OF TABLES

Table 2.1. Chemical constituents of red mud in different locations (%wt)	12
Table 2.2. Buffering common reactions in aqueous solution of bauxite residue.....	13
Table 2.3. Dissolution reactions of common buffering solids present in bauxite residues.....	14
Table 2.4. Summary of CO ₂ amount captured in previous studies on RM carbonation	41
Table 2.5. Reactions taking place in the carbonation of red mud	43
Table 3.1. Major mineral composition of raw RM	49
Table 3.2. Concentration of raw RM and liquor	61
Table 4.1. Comparison between rapid and long term ANC for RM	65
Table 4.2. Metal concentrations in RM liquor at different pH values	66
Table 4.3. Effect of CO ₂ concentrations on the composition of solid phase in carbonated RM as quantified by XRD	88
Table 4.4. Effect of total gas flow rate on the composition of solid phase in carbonated RM as quantified by XRD	92
Table 4.5. Effect of stirring speed on the composition of solid phase in carbonated RM as quantified by XRD.....	94
Table 4.6. Major elemental composition (%w/w in average) of RM and carbonated RM at different concentrations of CO ₂ , TF of gas 200mL/min, stirring speed 250rpm	99
Table 4.7. Major compound composition (%w/w in average) of RM and carbonated RM at different concentrations of CO ₂ , TF of gas 200mL/min, stirring speed 250rpm	101
Table 4.8. Major elemental composition (%w/w in average) of RM and carbonated RM at 15%-60% CO ₂ , TF of 200mL/min, 250rpm in 5 days of carbonation.....	102
Table 4.9. Major compound composition (%w/w in average) of RM and carbonated RM at 15%-60% CO ₂ , TF of 200mL/min, 250rpm in 5 days of carbonation.....	103
Table 4.10. Major elemental composition (%w/w in average) of RM and carbonated RM at 30% CO ₂ concentration, 250rpm and different total gas flow rate.....	104

Table 4.11. Major compound composition (%w/w in average) of RM and carbonated RM at 30% CO ₂ concentration, 250rpm and different total gas flow rate.....	105
Table 4.12. Major element composition (%w/w in average) of RM and carbonated RM at 30% CO ₂ , TF of 200mL/min and different stirring speeds.....	107
Table 4.13. Major compound composition (%w/w in average) of RM and carbonated RM at 30% CO ₂ , TF of 200mL/min and different stirring speeds.....	107
Table 4.14. Major element composition (%w/w in average) of RM and carbonated RM at 30% CO ₂ , TF of 200mL/min, 250rpm and different solids concentrations..	108
Table 4.15. Major compound composition (%w/w in average) of RM and carbonated RM at 30% CO ₂ , TF of 200mL/min, 250rpm and different solids concentrations..	109
Table 4.16. Concentration of raw RM and liquor	123
Table 4.17. Solid precipitation/dissolution reactions in red mud model.....	125
Table 4.18. Solid dissolution/precipitation and liquid reactions in RM simulation	131
Table A-1. Rapid titration of RM by 0.1N HCl	165
Table A-2. Rapid titration of RM liquor to pH 4.5 by 0.1N HCl	166
Table A-3. Long-term titration of RM to pH 4.5 by 0.1N HCl.....	167
Table A-4. Long-term titration of RM to pH 6.0 by 0.1N HCl.....	168
Table A-5. Long-term titration of RM to pH 8.0 by 0.1N HCl.....	169
Table A-6. Long-term titration of RM to pH 10 by 0.1N HCl.....	170
Table A-7. Metal concentrations in RM liquor measured at different pH values....	171
Table A-8. Simulated metal concentrations in RM liquor at different pH values ...	171
Table B-1. Carbonation of RM at different CO ₂ concentrations and total gas flow rate of 100mL/min, stirring speed of 250rpm	179
Table B-2. Carbonation of RM at different CO ₂ concentrations and total gas flow rate of 100mL/min, stirring speed of 250rpm	180
Table B-3. Carbonation of RM at different CO ₂ concentrations and total gas flow rate of 200mL/min, stirring speed of 250rpm	181
Table B-4. Carbonation of RM at different CO ₂ concentrations and total gas flow rate of 200mL/min, stirring speed of 250rpm	182
Table B-5. Carbonation of RM at different CO ₂ concentrations and total gas flow rate of 300mL/min, stirring speed of 250rpm	183

Table B-6. Carbonation of RM at different CO ₂ concentrations and total gas flow rate of 300mL/min, stirring speed of 250rpm	184
Table B-7. Carbonation of RM at different CO ₂ concentrations and total gas flow rate of 400mL/min, stirring speed of 250rpm	185
Table B-8. Carbonation of RM at different CO ₂ concentrations and total gas flow rate of 400mL/min, stirring speed of 250rpm	186
Table B-9. Carbonation of RM by 30% CO ₂ concentrations, stirring speed of 250rpm and different total gas flow rate	187
Table B-10. Carbonation of RM by 30% CO ₂ concentrations, total gas flow rate of 200mL/min and different stirring speeds	188
Table B-11. Carbonation of RM by 30% CO ₂ concentrations, TF of 200mL/min, speeds of 250rpm and different solids concentrations in RM.....	189
Table B-12. Longer carbonation of RM at 15% - 30% CO ₂ concentrations, TF of 200mL/min and stirring speed of 250rpm.....	190
Table B-13. Longer carbonation of RM at 40% - 60% CO ₂ concentrations, TF of 200mL/min and stirring speed of 250rpm.....	190
Table B-14. Longer carbonation of RM at by 30% CO ₂ concentrations, stirring speed of 250rpm and different total gas flow rate.....	191
Table B-15. Longer carbonation of RM at by 30% CO ₂ concentrations, stirring speed of 250rpm, TF of 200mL/min and different solids concentrations in RM.....	191
Table B-16. Carbonation of RM liquor at different CO ₂ concentrations, total gas flow rate of 100mL/min and stirring speed of 250rpm	192
Table B-17. Carbonation of RM liquor at different CO ₂ concentrations, total gas flow rate of 100mL/min and stirring speed of 250rpm	193
Table B-18. Carbonation of RM liquor at different CO ₂ concentrations, total gas flow rate of 200mL/min and stirring speed of 250rpm	194
Table B-19. Carbonation of RM liquor at different CO ₂ concentrations, total gas flow rate of 200mL/min and stirring speed of 250rpm	195
Table B-20. Carbonation of RM liquor at different CO ₂ concentrations, total gas flow rate of 300mL/min and stirring speed of 250rpm	196
Table B-21. Carbonation of RM liquor at different CO ₂ concentrations, total gas flow rate of 300mL/min and stirring speed of 250rpm	197

Table B-22. Carbonation of RM liquor at different CO ₂ concentrations, total gas flow rate of 400mL/min and stirring speed of 250rpm	198
Table B-23. Carbonation of RM liquor at different CO ₂ concentrations, total gas flow rate of 400mL/min and stirring speed of 250rpm	199
Table D-1. Simulated carbonation of RM at different CO ₂ concentrations and total gas flow rate of 100mL/min	202
Table D-2. Simulated carbonation of RM at different CO ₂ concentrations and total gas flow rate of 200mL/min	202
Table D-3. Simulated carbonation of RM at different CO ₂ concentrations and total gas flow rate of 300mL/min	203
Table D-4. Simulated carbonation of RM at different CO ₂ concentrations and total gas flow rate of 400mL/min	203